ISSN 1063-7834, Physics of the Solid State, 2020, Vol. 62, No. 3, pp. 419–422. © Pleiades Publishing, Ltd., 2020.
Russian Text © The Author(s), 2020, published in Fizika Tverdogo Tela, 2020, Vol. 62, No. 3, pp. 369–372.

SUPERCONDUCTIVITY

Superconductivity in Thin Films of the Dirac Semimetal Cd_3As_2

A. B. Davydov[a, *], L. N. Oveshnikov[a, b], A. V. Suslov[c], A. I. Ril[d], S. F. Marenkin[d, e], and B. A. Aronzon[a]

[a] *Lebedev Physical Institute, Russian Academy of Sciences, Moscow, 119991 Russia*
[b] *National Research Center Kurchatov Institute, Moscow, 123182 Russia*
[c] *National High Magnetic Field Laboratory, Tallahassee, Florida, USA*
[d] *Kurnakov Institute of General and Inorganic Chemistry, Russian Academy of Sciences, Moscow, Russia*
[e] *National University of Science and Technology MISiS, Moscow, 119049 Russia*
**e-mail: sanyadav@yandex.ru*

Received October 28, 2019; revised October 28, 2019; accepted November 30, 2019

Abstract—Thin films of Dirac semimetal Cd_3As_2 about 100 nm thick made of single crystals of cadmium arsenide, prepared by direct fusion of the elements by vacuum–ampoule method, by vacuum–thermal sputtering/depostion have been studied. Temperature and magnetic field dependences of electrical resistance have been measured, which indicate the presence of a superconducting transition at a temperature from 0.2 to 0.6 K.

Keywords: Dirac semimetal, superconductivity, thin films
DOI: 10.1134/S1063783420030063

This work is devoted to the experimental observation of superconductivity in the Dirac semimetal Cd_3As_2 in thin films with a thickness of ~100 nm. Earlier we reported the observation of superconductivity in the films grown by magnetron sputtering [1]. In this work, the films were grown by vacuum–thermal sputtering/deposition from Cd_3As_2 bulk single crystals of the corresponding composition.

It was theoretically shown in [2, 3] that superconductivity can be observed in the Dirac semimetal Cd_3As_2. The Hamiltonian of the electron–electron interaction was introduced as the sum of inter- and intraorbital parts in these papers. It has been predicted that if the interorbital contribution is greater than the intraorbital one, then an unusual superconductivity phase can be realized, and, if it is less, then ordinary superconductivity is realized. However, the nature of the superconductivity has not been studied experimentally and the mechanism of superconducting pairing has not been determined.

Earlier in [4], the superconductivity was observed under pressure of up to 13 GPa at a crystal structure rearrangement at 3.5 GPa. In our work, as in the case in [1], we observed the transition to superconductivity without the application of external pressure and, accordingly, without any rearrangement of the crystal structure. The results on the surface superconductivity of semimetallic Cd_3As_2 single crystals were also obtained by the point contact method in [5–7]. However, this is an indirect method that requires the subtraction of large quantities whereas we managed to detect the superconductivity by the direct method of zero resistance.

Three samples of thin films were produced and measured to check for reproducibility. All three films were deposited onto a silicon substrate and showed close values of parameters. The parameters of the films were as follows: the resistance at room temperature was 2034, 2135, and 2289 Ω and the concentration of charge carriers determined by hall measurements were 3.2×10^{18}, 3.3×10^{18}, and 3.1×10^{18} cm^{-3}, respectively. Films with a thickness of about 100 nm were obtained of Cd_3As_2 bulk single crystals by vacuum–thermal sputtering/deposition. Details of the preparation of the films are presented below.

Polycrystalline samples of Cd_3As_2 were grown of the high-purity Cd and As elements by direct fusion by vacuum–ampoule method in vacuumed (~10^{-2} Pa) quartz ampoules coated with pyrolytic carbon. The synthesis was carried out in several stages (considering the volatility of As): heating to 620°C at 30°C/h and further holding at this temperature for 5 h; heating to 780°C (20°C/h) holding for 2 days to homogenize the melt; and ampoule cooling when the furnace is in the off mode. The received polycrystals were ground into powder and used to grow the single crystal in a vacuumed (~10^{-2} Pa) double quartz ampoule. The growth was carried out in a vertical electric furnace using directed crystallization by the Bridgman method: heating with constant rotation of the ampoule to a temperature of 735°C (by 15 K above the melting point of Cd_3As_2), holding the melt for 12 h, and then moving the bottom parts of the ampoule into the cold

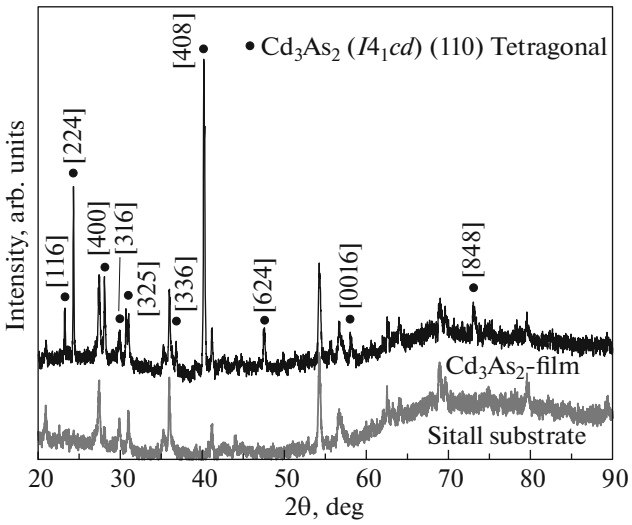

Fig. 1. Experimental X-ray diffraction patterns of the studied Cd_3As_2 film on a sitall substrate. The peaks present confirm the existence of only the α-Cd_3As_2 phase in the composition of the deposited film.

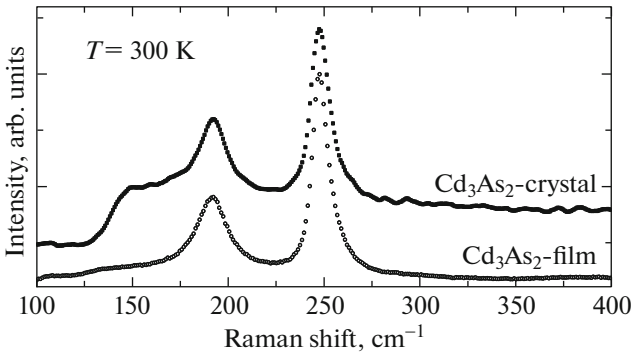

Fig. 2. The Raman shift of the curves for one of the Cd_3As_2 samples at room temperature and the Raman shift of the curves for the Cd_3As_2 single crystal at the same temperature, which has characteristic peaks at the points of 196 and 245 cm^{-1}.

zone at a speed of 0.7 mm/h at a furnace gradient of 1°C/cm. The phase composition of the polycrystals and single crystals obtained was analyzed using a powder diffractometer. Only the α-Cd_3As_2 phase (of space group $I4_1acd$) was present in the composition for both types of the crystals.

The residual vapor pressure in the chamber was maintained at the level of 1×10^{-4} Pa or less in the process of the deposition of the films. An annealing of a resistive type tungsten evaporator had been preliminarily performed and the crystals of the evaporated substance had been 1–2 mm in diameter. Silicon wafers [111] with dimensions of 3 × 5 mm were used as substrates. The distance between the evaporator and the substrates was 4 cm and the temperature of the substrates was 300 K. The film growth process was carried out until complete evaporation of the material, the mass of which was previously calculated to obtain films of the required thickness. The total deposition time was 8 min at a crystal mass of 0.05 g. The thickness of the films was 100 nm. The samples were prepared in the form of Hall bars, the linear dimensions of which were approximately 2 × 0.7 mm. Since the results obtained on all samples are close, only the one sample measurement data are presented below.

To determine the crystallographic structure of the films, the X-ray diffraction (XRD) measurements were performed on a similar sample but manufactured on a substrate of sitall. Some of the peaks from the substrate and from the film coincide when using a substrate of silicon, which significantly complicates the analysis of diffractograms. As a result, the peaks can be interpreted as peaks belonging to the α-phase of Cd_3As_2 of the space group $I4_1/acd$, the same as in the single crystal, except for the peaks corresponding to the substrate signals (Fig. 1), [8]. This pattern corresponds to the Dirac semimetal (DSM) [9]. The latter is also confirmed by Raman spectra, in which two bright peaks (196 and 245 cm^{-1}) are observed, completely corresponding to the position of the peaks of the Cd_3As_2 single crystal, as shown in Fig. 2.

The results of X-ray and Raman measurements prove good crystallographic quality of the grown samples, exceeding the quality of the films grown earlier by magnetron sputtering. The high quality of the samples is also confirmed by magnetoresistive measurements. The temperature dependence of the resistance of one of the three samples is shown in Fig. 3. All three samples studied in this paper show almost identical behavior in contrast to the samples obtained by the magnetron sputtering and showing a resistance spread of about 20–30%.

Magnetoresistive measurements were performed on a 20 T superconducting magnet in a dillution cryo-

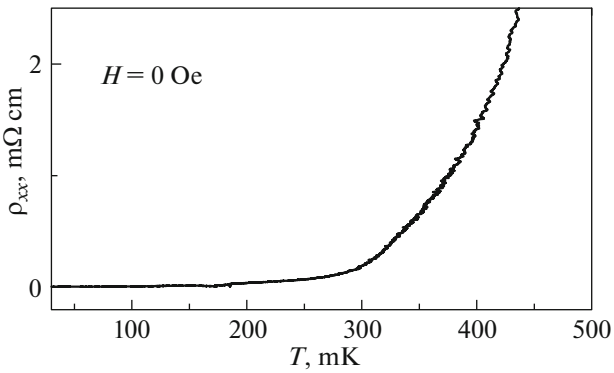

Fig. 3. Temperature dependences of the electrical resistance for the Cd_3As_2 sample. The curve unambiguously indicates the observed transition to superconductivity.

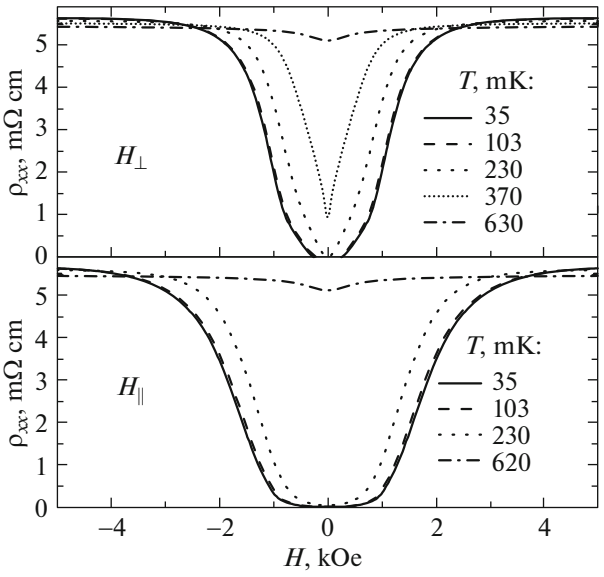

Fig. 4. Magnetic field dependences of the electrical resistance for two directions of the magnetic field, which was applied in the direction of 0° (magnetic field perpendicular to the plane of the sample, Fig. 4a) and 90° (magnetic field along the plane of the sample, perpendicular to the current, Fig. 4b) in the field up to 0.5 T. The numbers indicate the temperatures of the sample at which measurements were made.

stat equipped with a sample rotator, SCM1, located in National High Magnetic Field Laboratory, Tallahassee, USA. A sharp drop in the resistance at temperatures below 0.5 K and its further (below 0.2 K) turning to zero, indicating the transition of the sample into a superconducting state, is clearly visible in Fig. 3. The dependences of the electrical resistance on the magnetic field, which was applied in the direction of 0° (magnetic field perpendicular to the plane of the sample, Fig. 4a) and 90° (magnetic field along the plane of the sample, perpendicular to the current, Fig. 4b) in the field up to 0.5 T. The temperature from 0.035 K to 0.630 K was used as a parameter.

These figures show the transition from a normal half-metal state to the superconductivity. As you would expect, the transition curves are significantly narrower from about 0.2 to 0.015 T in the case of a magnetic field directed perpendicular to the sample plane. If, in turn, the magnetic field lies in the plane of the sample, the transition curves are wider 0.3–0.05 T. This corresponds to a greater value of the critical field H_c, which is a common property for all thin superconducting films. Both Figs. 4a and 4b clearly testify to the phase transition to superconductivity.

According to our original hypothesis, the appearance of superconductivity in our samples is due to the influence of the substrate. We assumed that the compression of the substrate during cooling is transferred to the sample (as the temperature decreases), which is

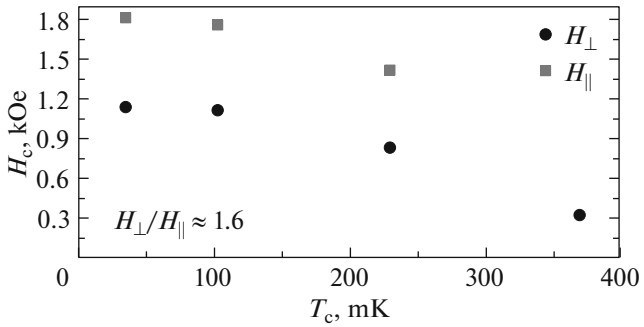

Fig. 5. The H_c–T_c phase diagram constructed for $\alpha = 1$ and $\beta = 1$ according to Eq. (1), which corresponds to the Ginzburg–Landau theory.

equivalent to the sample being under pressure, as in [4]. We examined Cd_3As_2 films grown on various substrates: Si, Al_2O_3, and Sitall to test this assumption. The analysis showed that the temperature coefficient of expansion of Cd_3As_2 was greater than the temperature coefficient of expansion of the substrate in all cases, in other words, the sample was effectively stretched rather than compressed, and therefore we had to exclude the pressure version. Moreover, it was observed experimentally that the temperature of the superconducting transition T_c decreased to zero with a decrease in the temperature coefficient of expansion of the substrate, which contradicts the assumption of sample compression and does not allow the analogy with the case described in [4].

We obtained the H_c–T_c diagrams for the samples studied, shown in Fig. 5. These diagrams correspond to the characteristic ratio

$$H(T) = H_c(0)[1 - (T/T_c)^\alpha]^\beta, \qquad (1)$$

where α and β are coefficients and H_c is the critical magnetic field. According to the Bardeen–Cooper–Schrieffer theory (BCS), $\alpha = 2$ and $\beta = 1$ near zero temperature. At the same time, according to the Ginzburg–Landau theory (GL), $\alpha = 1$ and $\beta = 1$ for the description of the temperature dependence near T_c and near the critical field H_{c2} when considering II-type superconductivity. However, the same linear dependence is applicable in our case, in the intermediate temperature range, that is, beyond the strict applicability of the Ginzburg–Landau theory (see Fig. 5).

Thus, the H_c–T_c graphs correspond to linear behavior in the intermediate temperature range, similar to Cd_3As_2 and Bi_2Se_3 bulk crystals under a pressure of 13 GPa application. According to the M. Sato and Y. Ando theory [3], as well as to the results in [4–7], triplet electron pairing is most likely at a pressure of 13 GPa or at a surface conductivity observed by a point contact. We can only assume that nontrivial p-type pairing occurs in the studied films also in our case.

Thus, it can be argued that the presence of superconductivity in the absence of external overpressure is proved in thin films of the Dirac semimetal Cd_3As_2.

ACKNOWLEDGMENTS

The authors thank K.I. Kugel for useful discussions.

FUNDING

The work was performed with the support of RSF project no. 17-12 01345. The national laboratory of strong magnetic fields (NHMFL, USA) is funded by the National Science Foundation (grant NSF/DMR-1644779) and the state of Florida.

CONFLICT OF INTEREST

The authors state that they have no conflicts of interest.

REFERENCES

1. A. V. Suslov, A. B. Davydov, L. N. Oveshmikov, L. A. Morgun, K. I. Kugel, V. S. Zakhvalinskii, E. A. Pilyuk, A. V. Kochura, A. P. Kuzmenko, V. M. Pudalov, and B. A. Aronzon, Phys. Rev. B **99**, 094512 (2019).
2. S. Kobayashi and Y. Sato, Phys. Rev. B **94**, 014510 (2016).
3. M. Sato and Y. Ando, Rep. Prog. Phys. **80**, 076501 (2017).
4. L. He, X. Hong, S. Li, Y. Jia, S. Zhang, and C. Jin, npj Quantum Mater. **1**, 16014 (2016).
5. H. Wang, H. Wang, H. Liu, H. Lu, W. Yang, S. Jia, X.-J. Liu, X. C. Xie, J. Wei, and J. Wang, Nat. Mater. **15**, 38 (2015).
6. L. Aggarwal, A. Gaureav, G. S. Thakure, Z. Haque, A. K. Ganguli, and G. Sheet, Nat. Mater. **15**, 32 (2015).
7. O. O. Shvetsov, V. D. Esin, A. V. Timonina, N. N. Kolesnikiv, and E. V. Deviatov, Phys. Rev. B **99**, 125305 (2019).
8. E. Arushanov, Prog. Cryst. Growth Charact. Mater. **3**, 211 (1981).
9. N. P. Armitage, E. J. Mele, and A. Vishwanath, Rev. Mod. Phys. **90**, 015001 (2018).

Translated by N. Petrov